Journal of Molecular Structure 1293 (2023) 136278

Contents lists available at ScienceDirect

Journal of Molecular Structure

journal homepage: www.elsevier.com/locate/molstr

The stable conformations and vibronic and cation spectroscopy of 2-ethoxybenzonitrile

Shuxian Li [a], Yan Zhao [b], Fuqiang Hu [a], Yuechun Jiao [a,c], Jianming Zhao [a,c], Changyong Li [a,c,*]

[a] State Key Laboratory of Quantum Optics and Quantum Optic Devices, Institute of Laser Spectroscopy, Shanxi University, Taiyuan, Shanxi 030006, China
[b] Department of Physics and Electronics Engineering, Jinzhong University, Jinzhong, Shanxi 030619, China
[c] Collaborative Innovation Center of Extreme Optics, Shanxi University, Taiyuan, Shanxi 030006, China

ARTICLE INFO

Keywords:
2-ethoxybenzonitrile
Conformer
Cation
REMPI
MATI
Franck-Condon simulation

ABSTRACT

Ethoxy-substituted benzene has several stable conformations as the single bond in the ethoxy group is capable of internal rotation. Ethoxybenzonitrile may has more conformers due to different orientations of ethoxy with respect to the CN group. In this paper, the potential energy surface (PES) of 2-ethoxybenzonitrile in the ground state was calculated at the level of B3LYP/cc-pvdz, and five different molecular conformers were found on the PES. Only the most stable conformer I (trans) was observed in the supersonic molecular beam experiments. The resonance enhanced multiphoton ionization (REMPI) and mass analyzed threshold ionization (MATI) spectra of 2-ethoxybenzonitrile were measured and Franck-Condon simulations were performed, and the theoretical results are in good agreement with the experimental measurements. The similar molecular structures in S_0, S_1, and D_0 states imply the large Franck-Condon factors. The vibronic structures in S_1 and D_0 states were analyzed in detail and the vibronic features were assigned. The MATI spectra follow well the propensity rule $\Delta v = 0$, indicating that the molecular structures of the cationic and excited states are similar. Most of the observed vibrations are associated with the ring in-plane distortion. The band origin of the $S_1 \leftarrow S_0$ transition and the accurate adiabatic ionization energy of 2-ethoxybenzonitrile are determined for the first time to be 34 092 ± 2 and 69 796 ± 5 cm^{-1}, respectively.

1. Introduction

The ethoxy group has a longer chain relative to methyl, ethyl, or methoxy, leading to the possibility of many different conformers for its substituted benzene derivatives. Many researches on the derivatives of ethoxybenzene (or phenetole) have been reported. In 2003, Cinacchi and Prampolini calculated the internal rotational potential energy of ethoxybenzene and ethylbenzene with the theory of B3LYP/6–311G(2d, p), which shows that the molecular potential energy is minimal when the chain is in the plane of ring, and in trans position with respect to the O—CH_2 linkage [1]. In 2006, the laser-induced fluorescence excitation and dispersed fluorescence spectra of phenetole were measured by Ramanathan et al. [2]. They combined with different theoretical calculations to confirm that there is only one conformer existing in supersonic jet. In 2010, Egawa et al. studied the conformational properties of phenetole by laser-jet spectroscopy and performed the quantum-mechanical analysis of the two-dimensional potential energy surfaces (PES) for S_0 and S_1 states [3]. It is proposed that in addition to the trans configuration, another configuration gauche maybe exist in supersonic jet. In 2016, Ferres et al. measured and assigned the microwave spectroscopy of phenetole in the supersonic molecular beam, and combined with the quantum-chemical calculations to study the molecular structure [4]. They also concluded that phenetole has two conformers: trans and gauche. The gauche conformer has the ethyl tilted out of the phenyl plane by about 70°, but only the trans configuration was observed in the gas phase. In 2019, the vibrational spectra of the first electronically excited state and cationic ground state of phenetole were measured by Helle et al. with resonance enhanced multiphoton ionization (REMPI) and mass analyzed threshold ionization (MATI) techniques, and the $S_1 \leftarrow S_0$ transition energy and the adiabatic ionization energy (IE) of phenetole were determined to be 36 370 ± 4 and 65 665 ± 7 cm^{-1}, respectively [5]. Two signals at low frequency direction of the 0^0 band were observed in the REMPI spectrum, and considered to be two other isomer's origin bands probably. However, these two signals were not as abundant and not be analyzed any further. They also analyzed the effect of molecular side chains by comparing the experimental results

* Corresponding author.
E-mail address: lichyong@sxu.edu.cn (C. Li).

https://doi.org/10.1016/j.molstruc.2023.136278
Received 18 March 2023; Received in revised form 6 July 2023; Accepted 22 July 2023
Available online 22 July 2023

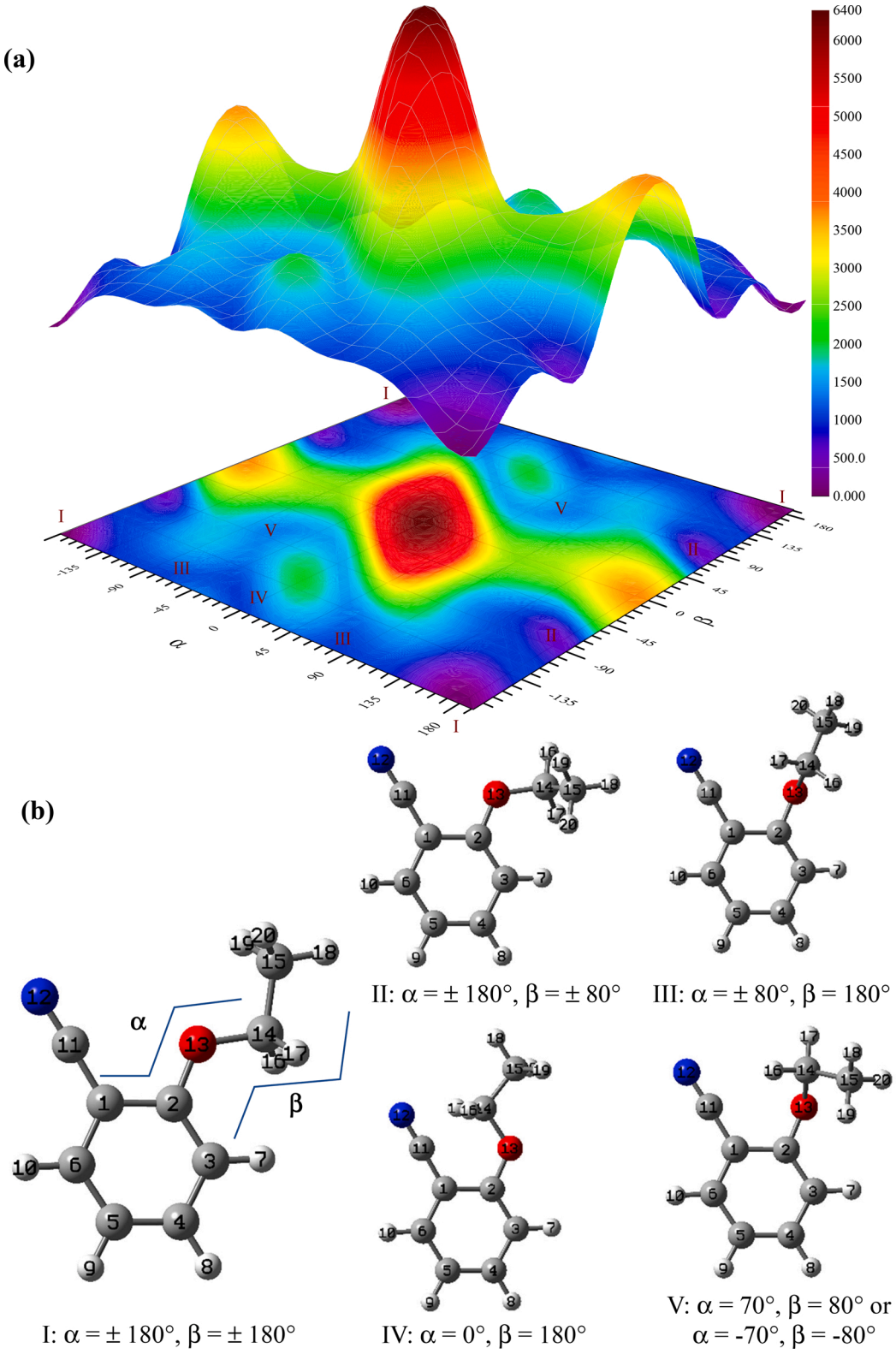

Fig. 1. (a) Potential energy surface (PES) calculated at B3LYP/cc-pvdz level for the ground state S_0 of 2-ethoxybenzonitrile. The dihedral angle ∠C1C2O13C14 (α) and ∠C2O13C14C15 (β) are used as the scanning variables. (b) Five conformers corresponding to five different locate minimums as marked on the PES. The relative energies of conformers I, II, III, IV, and V further calculated at the level of B3LYP/aug-cc-pvtz are 0, 600, 957, 1016, and 1306 cm^{-1}, respectively.

with anisole.

At present, many molecules have been deeply studied by REMPI, MATI, and ZEKE spectroscopy, and there are also many reports on benzonitrile derivatives [6–13]. As far as we know, however, it is very less on 2-ethoxybenzonitrile researches. In this paper, the potential energy surface of the neutral ground state of 2-ethoxybenzonitrile was calculated at the level of B3LYP/cc-pvdz, and five different molecular conformers were found. The most stable conformer was confirmed at the

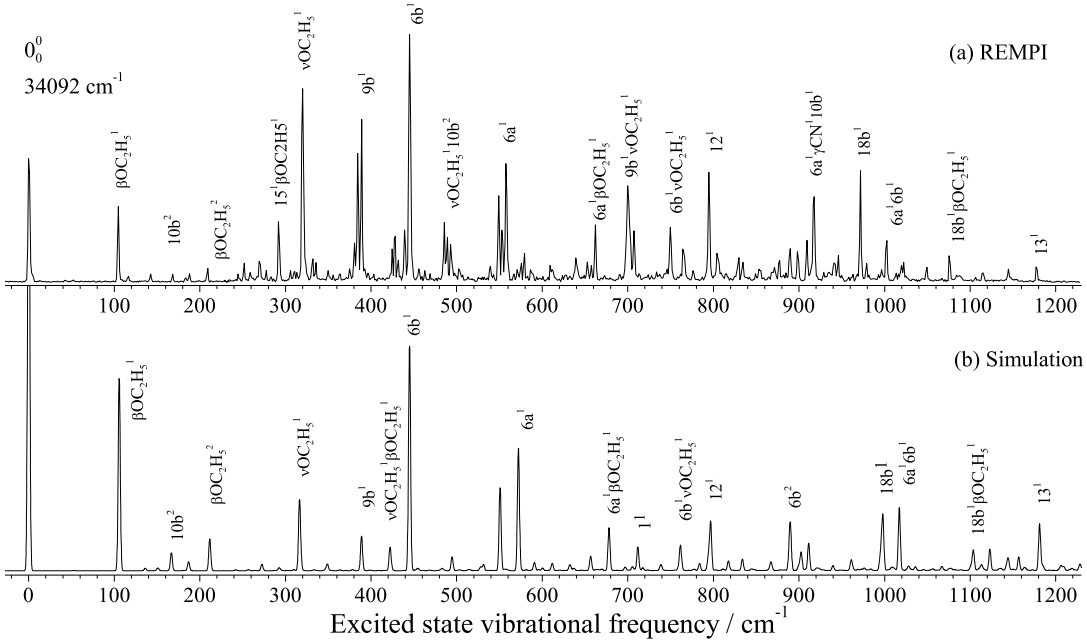

Fig. 2. (a) Two-color REMPI spectra of 2-ethoxybenzonitrile. (b) Franck-Condon simulation at B3LYP/aug-cc-pvtz level.

supersonic molecular beam. The REMPI and MATI spectra of the molecule were measured and simulated. The vibronic structures in S_1 and D_0 states were analyzed in detail. The MATI spectra follow well the propensity rule $\Delta\nu = 0$, indicating that the molecular structures of the cationic ground state and excited state are similar.

2. Experiment and computation

2.1. Experiment

The 2-ethoxybenzonitrile sample was purchased from Aladdin and used without further purification. It is a colorless or faint yellow liquid with a purity of 98%. The sample was heated to about 150 °C to obtain sufficient vapor pressure. 3 bar krypton gas was used as the carrier gas and carried the sample molecules into the beam source chamber through a pulse valve of 0.5 mm diameter nozzle. And then, the molecule beam entered the ionization chamber through a skimmer located 20 mm downstream from the nozzle orifice. The vacuum pressures of the source chamber and ionization chamber are $\sim 10^{-4}$ Pa and $\sim 10^{-6}$ Pa, respectively.

The laser system consists of two sets of YAG laser pumped dye lasers. The first dye laser (CBR-D-24, Sirah) pumped by a frequency-doubled Nd: YAG laser (Qsmart 850) was used as the excitation laser. The second dye laser (Precision Scan-D, Sirah) pumped by another frequency-tripled Nd: YAG laser (Qsmart 850) was used as the ionization laser for REMPI or probe laser for MATI. The dyes of pyrromethene 597 and coumarin 540A were used for the excitation and ionization laser, respectively. The output wavelengths were calibrated by a wavemeter (WS7–60 UV-I).

Due to the strong electron-withdrawing ability of the cyano group, benzonitrile derivatives have higher ionization energies. For many of them, the transition energy of $S_1 \leftarrow S_0$ is lower than that of $D_0 \leftarrow S_1$. Such an energy structure indicates that a two-color REMPI experiment is required for the excited state spectrum. In this experiment, we fixed the ionization laser at 261.25 nm, then scan the excitation laser from 283 to 293.5 nm to obtain the vibronic spectrum of the first electronically excited state S_1.

In the MATI experiment, the molecule in ground state is resonantly excited to specific vibronic levels in the S_1 state, then excited to the high Rydberg state by the probe laser. A −0.5 V/cm pulsed electric field was applied to remove the prompt ions. After a time delay of about 30 μs, the Rydberg molecules were ionized by a 140 V/cm pulsed electric field. Newly formed threshold ions pass through a 48 cm field-free region to be detected by a Microchannel plates (MCP) detector. The signal was collected by SR430 and recorded by a computer. The time sequence of the whole system is controlled by a pulse delay generator (SRS: DG645). More details about the experimental system have been described in our previous publications [14–17].

2.2. Computational method

All calculations were performed using the GAUSSIAN 16 program package [18]. The Becke three-parameter functional with the Lee−Yang−Parr functional (B3LYP) was chosen to perform density functional theory (DFT) calculations. The potential energy surface (PES) was calculated at the level of B3LYP/cc-pvdz, which yield the best solution for accuracy and computational costs. The geometry optimization, vibrational frequencies of S_0, S_1, and D_0 states were calculated at the levels of RB3LYP/aug-cc-pvtz, TD-B3LYP/aug-cc-pvtz, and UB3LYP/aug-cc-pvtz, respectively. The vibrational frequencies calculated at the (TD)-B3LYP/aug-cc-pvtz level were scaled by 0.984 and 0.983 for S_1 and D_0 states, respectively, so as to correct the deviations resulting from the neglect of anharmonic effects, the incomplete treatment of electron correlation, and the use of a finite basis set. Before the experiments, we need to first estimate the approximate value of ionization energy (IE) in order to select the appropriate laser dye. G4 and CBS-QB3 methods were used to predict the IEs, which yield more precise IE than DFT. Generally, the relative error of G4 and CBS-QB3 method is about one order of magnitude lower than that of DFT theory. The spectral simulations were performed based on the above DFT calculations. Combining with the theoretical calculations and simulated spectra, the vibronic spectra measured by REMPI and MATI experiments were assigned.

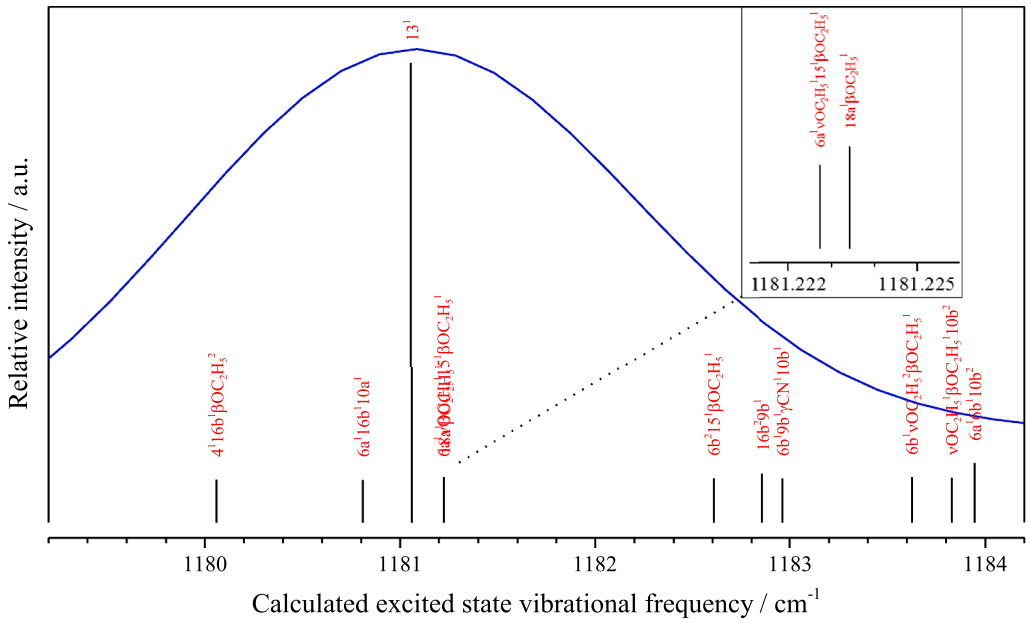

Fig. 3. Franck-Condon simulation spectrum and the band components near 1181 cm^{-1}. The insert shows two modes with almost equal frequencies.

Table 1
Vibrational frequencies (in cm^{-1}) and assignments of the observed bands in the two-color REMPI experiment of 2-ethoxybenzonitrile.

Exp.[a]	Calc.	Assignment [b]
105	106	$\beta OC_2H_5^1$
168	166	$10b^2$
209	212	$\beta OC_2H_5^2$
292	293	$15^1\beta OC_2H_5^1$
320	316	$\nu OC_2H_5^1$
384	378	$10b^2\beta OC_2H_5^2$
389	389	$9b^1$
428	423	$\nu OC_2H_5^1\beta OC_2H_5^1$
445	445	$6b^1$
486	483	$\nu OC_2H_5^1 10b^2$
549	551	$6b^1\beta OC_2H_5^1$
558	572	$6a^1$
579	591	βCN^1
609	612	$6b^1 10b^2$
639	633	$\nu OC_2H_5^2$
662	678	$6a^1\beta OC_2H_5^1$
700	697	$9b^1\nu OC_2H_5^1$
707	712	1^1
750	762	$6b^1\nu OC_2H_5^1$
764	778	$9b^2$
795	797	12^1
804	811	$9b^1\nu OC_2H_5^1\beta OC_2H_5^1$
830	834	$6b^1 9b^1$
890	890	$6b^2$
898	902	$12^1\beta OC_2H_5^1$
909	911	$\nu O—C_2H_5^1$
918	921	$6a^1\gamma CN^1 10b^1$
946	961	$6a^1 9b^1$
972	998	$18b^1$
1003	1017	$6a^1 6b^1$
1075	1077	$6b^2 15^1$
1115	1123	$6a^1 6b^1\beta OC_2H_5^1$
1145	1157	$1^1 6b^1$
1177	1181	13^1

[a] The experimental values are shifts from 34 092 cm^{-1}, whereas the calculated ones are obtained from the TD-B3LYP/aug-cc-pvtz calculation, scaled by 0.984.
[b] ν, stretching; β, in-plane bending; γ, out-of-plane bending.

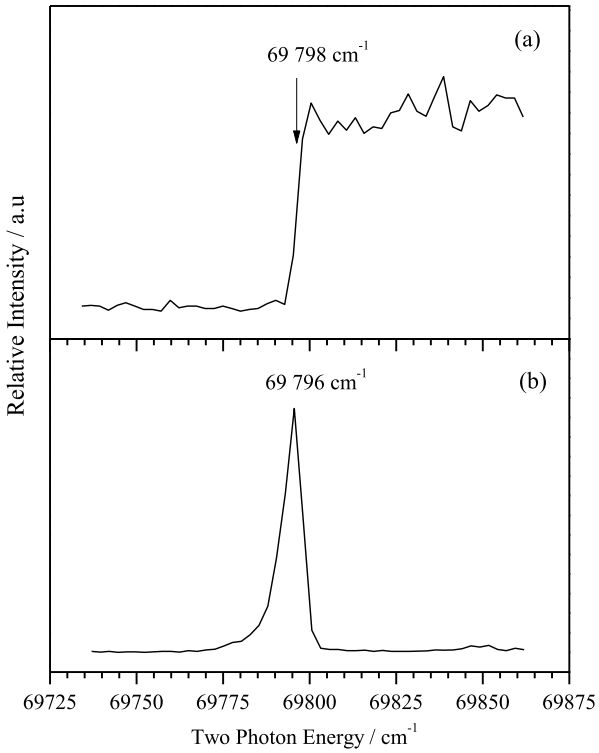

Fig. 4. (a) PIE curve of 2-ethoxybenzonitrile, (b) MATI spectrum via the $S_1 0^0$ intermediate.

3. Results and discussion

3.1. Calculated conformers and ionization energies

2-ethoxybenzonitrile is formed by the substitution of two ortho-position hydrogen atoms of the benzene molecule with ethoxy and cyano groups, respectively. The cyano group is always located in the ring plane in the stable configurations, and the ethoxy group probable orientation determines the number of stable conformers. In previous

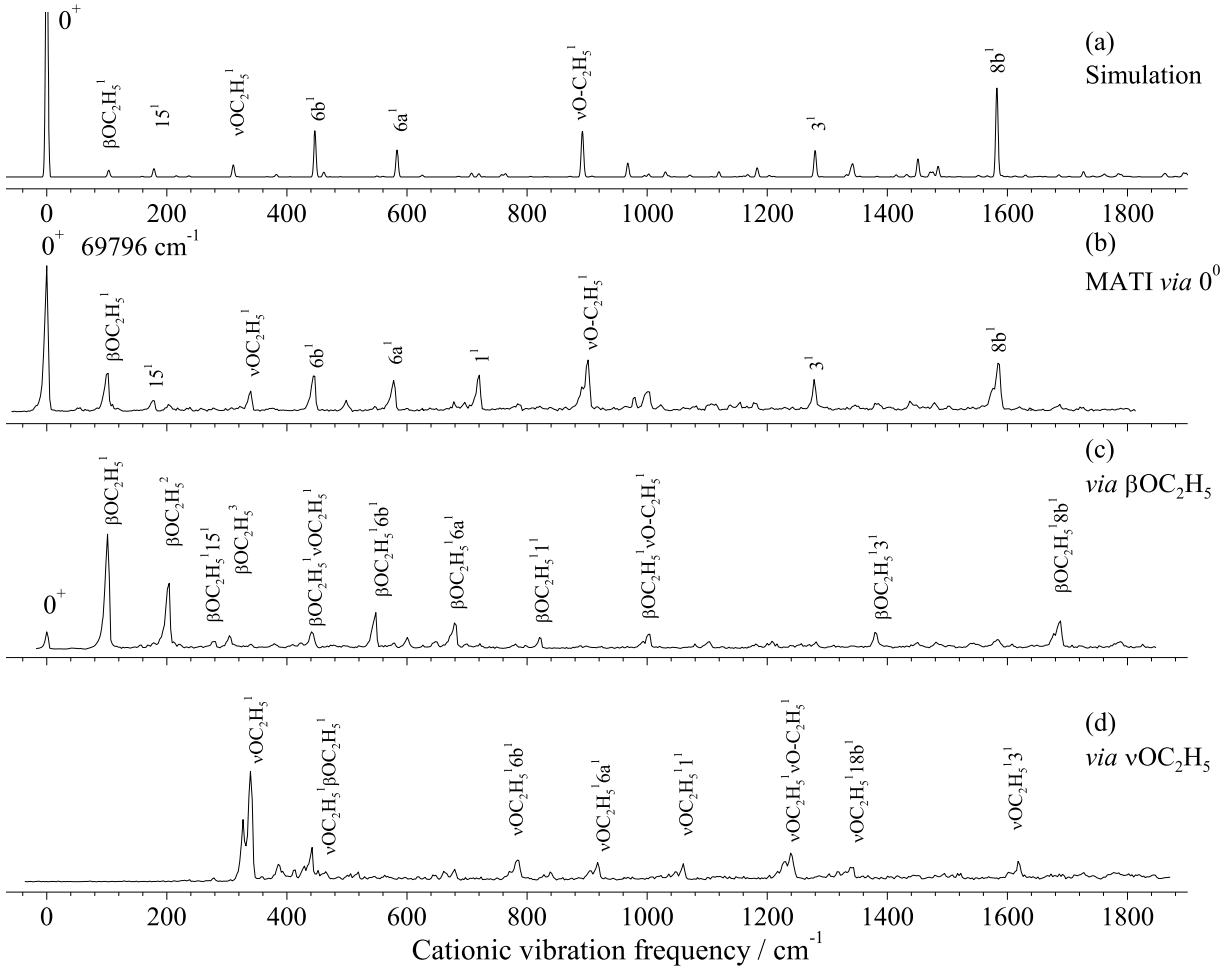

Fig. 5. Franck-Condon simulation spectrum of the cationic ground state D_0 at the level of B3LYP/aug-cc-pvtz (a), and the MATI spectra via $S_1 0^0$ (b), $S_1 \beta OC_2H_5$ (c), and $S_1 \nu OC_2H_5$ (d) intermediate states.

studies on ethoxybenzene, there were many different conclusions about the orientation of the ethoxy group with respect to the ring [3–5]. In this paper we scan the two dihedral angles of ∠C1C2O13C14 (α) and ∠C2O13C14C15 (β) with a step size of 10° to yield the potential energy surface (PES) of 2-ethoxybenzonitrile in S_0 state at the level of B3LYP/cc-pvdz as shown in Fig. 1(a), and the atomic labels are shown in Fig. 1(b). It is clear that at β = 0° the energy is high, there is not any minimum. At α = ± 180° there are two different local minimums I and II, and at β = ± 180° there are three different local minimums I, III, and IV. At α = 70°, β = 80° or α = −70°, β = −80° we can find the last minimum V. These minimums have been marked in Fig. 1(a). As a result, a total of five different local minimums were found on the PES, which correspond to five conformers of 2-ethoxybenzonitrile, tentatively named conformer I (trans), II (trans-gauche), III, IV (*cis*), V (cis-gauche), respectively. The structures are shown in Fig. 1(b). The further geometry optimizations at the level of B3LYP/aug-cc-pvtz show that the relative energies of five conformations I, II, III, IV, and V are 0, 600, 957, 1016, and 1306 cm^{-1}, respectively. We can estimate the relative abundances of the conformers according to the formula, $D2/D1 = \exp(-\Delta E/kT)$, where ΔE is the relative energy between the conformer 2 and conformer 1, T is the nozzle temperature in Kelvin, and Di is the Density of conformer i [19–23]. So, we know that the relative abundances with a nozzle temperature of 423 K (the experimental conditions for this paper) are 1, 0.13, 0.04, 0.03, and 0.01 for conformer I to V, respectively. It is clear that except for conformer I, which has a Cs symmetry, other conformers are very less. A lot of experiments show that if one conformer is ~300 cm^{-1} higher than the lowest conformer in energy, it would not be observed in the supersonic molecular beam. This means that just one conformer I (trans) can be observed in our experiment, because the other four configurations are too high in energy and too less in molecular density resulting in too weak signals to be detected. This is very similar to the case of ethoxybenzene [1,2,5].

The theoretical IE is deduced from the energy difference between the D_0 and S_0 states at $T = 0$ K. The calculated energies of D_0 and S_0 states by CBSQB3 method are −477.186423 and −477.505503 hartree, respectively, and it gives an IE value of 70 030 cm^{-1}. Similarly, the calculated energies of D_0 and S_0 states by G4 are −477.742629 and −478.061702 hartree, respectively, and it gives an IE value of 70 028 cm^{-1}. The IE relative deviations with CBS-QB3 and G4 theories from the experimental value are 0.340% and 0.337%, respectively. The calculated results are in good agreement with the experimental value, which provide an important reference for selecting a suitable dye.

3.2. *REMPI spectra*

The excited state spectrum of the $S_1 \leftarrow S_0$ transition of 2-ethoxybenzonitrile measured by two-color REMPI experiment with the vibration frequency range of 0 – 1228 cm^{-1} is shown in Fig. 2(a), and its Franck-Condon simulation spectrum calculated at level of B3LYP/aug-cc-pvtz is shown in Fig. 2(b). It can be seen that the experimental result is in good agreement with the calculated one. The spectral simulation reveals the components of spectral bands, and it is very helpful for the spectral assignment. Fig. 3 shows the Franck-Condon simulation spectra near 1181 cm^{-1}. We can find that the band at 1181 cm^{-1} is composed of

Table 2
Experimental and calculated vibrational frequencies (in cm^{-1}) and assignments of 2-ethoxybenzonitrile in the cationic ground state D_0.

Vibration frequency[a]			Calc.	Assignment [b]
0^0	$\beta OC_2H_5^1$	$\nu OC_2H_5^1$		
102	102		103	$\beta OC_2H_5^1$
177			179	15^1
205	204			$\beta OC_2H_5^2$
	281		282	$15^1\beta OC_2H_5^1$
	304			$\beta OC_2H_5^3$
		327	329	$\gamma CN^1\gamma C_2H_5^1$
340		340	311	$\nu OC_2H_5^1$
	441	442		$\beta OC_2H_5^1\nu OC_2H_5^1$
444			447	$6b^1$
499				$16b^1\gamma OC_2H_5^1$
	548			$\beta OC_2H_5^16b^1$
578			583	$6a^1$
		679		$\nu OC_2H_5^2$
	679			$\beta OC_2H_5^16a^1$
720			720	1^1
		784		$\nu OC_2H_5^16b^1$
	821			$\beta OC_2H_5^11^1$
902			893	$\nu O—C_2H_5^1$
		917		$\nu OC_2H_5^16a^1$
977			968	$\nu CH_2—CH_3^1$
1001			1003	$18b^1$
	1004			$\beta OC_2H_5^1\nu O—C_2H_5^1$
		1060	1060	$\nu OC_2H_5^11^1$
		1239		$\nu OC_2H_5^1\nu O—C_2H_5^1$
1278			1279	3^1
		1338		$18b^1\nu OC_2H_5^1$
	1379			$\beta OC_2H_5^13^1$
			1451	$19b^1$
1584			1583	$8b^1$
		1618		$\nu OC_2H_5^13^1$
	1688			$\beta OC_2H_5^18b^1$

[a] The experimental values are shifts from 69 796 cm^{-1}, whereas the predicted ones are obtained from the B3LYP/aug-cc-pvtz calculation, scaled by 0.983.
[b] ν, stretching; β, in-plane bending; γ, out-of-plane bending.

Table 3
Geometric parameters of rotamer I (trans) of 2-ethoxybenzonitrile in the S_0, S_1, and D_0 states, calculated at B3LYP/aug-cc-pvtz level.

	S_0	S_1	D_0	$\Delta(S_1\text{-}S_0)$	$\Delta(D_0\text{-}S_1)$
Bond length /Å					
C_1—C_2	1.411	1.454	1.456	0.043	0.002
C_2—C_3	1.395	1.401	1.423	0.006	0.022
C_3—C_4	1.39	1.415	1.366	0.025	−0.048
C_4-C_5	1.389	1.403	1.419	0.014	0.016
C_5-C_6	1.386	1.408	1.395	0.022	−0.012
C_6-C_1	1.396	1.42	1.383	0.023	−0.036
C_1-C_{11}	1.427	1.396	1.416	−0.030	0.020
C_{11}-N_{12}	1.153	1.167	1.154	0.014	−0.012
C_2-O_{13}	1.348	1.333	1.293	−0.014	−0.039
O_{13}-C_{14}	1.433	1.441	1.484	0.008	0.043
C_{14}-C_{15}	1.512	1.511	1.505	−0.001	−0.005
C_{14}-H_{16}	1.094	1.092	1.089	−0.001	−0.001
C_{14}-H_{17}	1.094	1.092	1.089	−0.001	−0.001
C_{15}-H_{18}	1.090	1.090	1.090	0	0
C_{15}-H_{19}	1.089	1.089	1.088	0	0
C_{15}-H_{20}	1.089	1.089	1.088	0	0
C_3-H_7	1.078	1.078	1.079	0	0
C_4-H_8	1.082	1.078	1.081	−0.003	0.003
C_5-H_9	1.08	1.082	1.081	0.002	0
C_6-H_{10}	1.081	1.079	1.080	−0.001	0.001
Bond angle /°					
$C_2C_1C_{11}$	120.1	120.8	118.9	0.7	−1.8
$C_1C_{11}N_{12}$	178.4	178.2	179.6	−0.2	1.4
$C_1C_2O_{13}$	116.1	113.2	115.1	−3.0	2.0
$C_2O_{13}C_{14}$	119.6	122.1	123.7	2.5	1.6
$O_{13}C_{14}C_{15}$	107.6	107.7	107.4	0.1	−0.4
Dihedral angle /°					
$C_3C_2O_{13}C_{14}$	0	0	0	0	0
$C_2O_{13}C_{14}C_{15}$	180.0	180.0	180.0	0	0

many vibrational modes, except for mode 13^1 which is the main contributor for the band, others belong to the combined vibrations. Some frequencies of them are almost equal, such as the two vibrational modes enlarged in the insert of Fig. 3. The obvious feature of both REMPI and its simulation in Fig. 2 is that the rate of signal-to-noise in low frequency region is greater than that in high frequency region. The simulation spectrum shows that the spectral band in high frequency region is composed of many components, including fundamental, overtone, and combination of various vibrations. So numerous weak and dense components raise the spectral baseline and result in the bad rate of signal-to-noise in high frequency region. For simplicity's sake, we only list the largest contributor to the observed bands in Table 1.

Based on DFT calculation, spectral simulation, and previous publication on 2-methoxybenzonitrile [8], we analyzed and assigned the vibronic spectra of 2-ethoxybenzonitrile. The labeling convention of the vibrational modes follows the Varsanyi's system [24], which is based on the Wilson's notation [25]. The band at 34 092 cm^{-1} is assigned as the origin of the S_1←S_0 transition. Many ring in-plane vibrations are observed, such as the bands at 389, 445, 558, 707, 795, 972 and 1177 cm^{-1} are assigned to the ring deformations $9b^1$, $6b^1$, $6a^1$, 1^1, 12^1, $18b^1$, and 13^1, respectively. Several in-plane vibrations of the ethoxy group are active, such as OC_2H_5 in-plane bending βOC_2H_5 and stretching νOC_2H_5 appearing at 105, and 320 cm^{-1}, respectively. These fundamental modes have greater Franck-Condon factors and stronger signals in the REMPI spectrum. Other bands observed in REMPI spectrum are assigned to overtones and combination vibrations of several modes. Such as the bands at 168, 209, 639, 764 and 890 cm^{-1} are assigned as $10b^2$, $\beta OC_2H_5^2$, $\nu OC_2H_5^2$, $9b^2$, and $6b^2$, respectively. The rest of the bands are weak and assigned as the combined vibrations of several modes. The experimental frequencies, calculated frequencies, and possible assignments are listed in Table 1.

3.3. PIE and MATI spectra

To obtain the detailed information on the cationic ground state D_0, we measured the PIE and MATI spectra. Fig. 4(a) shows the PIE curve of 2-ethoxybenzonitrile recorded via the $S_1 0^0$ (34 092 cm^{-1}) intermediate state. The rising step yields the approximate value of the adiabatic ionization energy to be 69 798 cm^{-1} with an uncertainty of 10 cm^{-1}. PIE spectrum provides an important reference for MATI experiments. As a comparison, we also show the MATI spectrum via $S_1 0^0$ intermediate state in Fig. 4(b), which provides a more precise IE of 69 796 ± 5 cm^{-1}.

Fig. 5(a) is the Franck-Condon simulation spectrum of D_0←S_1 transition calculated at the level of B3LYP/aug-cc-pvtz, and (b), (c), (d) are the experimental MATI spectra via the $S_1 0^0$, $S_1\beta OC_2H_5^1$ (105 cm^{-1}) and $S_1\nu OC_2H_5^1$ (320 cm^{-1}) intermediate states, respectively. MATI spectra provide more accurate cationic data with high signal-to-noise ratio than PIE. Since the MATI experiment applied a pulsed electric field of - 0.5 V/cm to remove the prompt ions, the measured IE is less $4*F^{1/2}$ than the real value. This derivation due to Stark effect has been corrected for present results.

In the MATI spectrum via $S_1 0^0$, most of the observed modes are due to in-plane deformation of the ring. As shown in Fig. 5(b), the most intense peak is assigned as the origin 0^+ of the D_0←S_1 transition of 2-ethoxybenzonitrile, and the adiabatic IE is determined to be 69 796 ± 5 cm^{-1}. The bands at 177, 444, 578, 720, 1001, 1278 and 1584 cm^{-1} are all due to the fundamental vibration of the benzene ring, which are assigned as 15^1, $6b^1$, $6a^1$, 1^1, $18b^1$, 3^1 and $8b^1$, respectively. The bands at 102, 340, 902, and 977 cm^{-1} are the vibrations from substituents, and are assigned as $\beta OC_2H_5^1$, $\nu OC_2H_5^1$, $\nu O—C_2H_5^1$, and $\nu CH_2—CH_3^1$, respectively. The bands at 205 and 499 cm^{-1} are assigned to overtone $\beta OC_2H_5^2$ and combination vibration $16b^1\gamma OC_2H_5^1$, respectively.

When the $S_1\beta OC_2H_5^1$ (105 cm^{-1}) is used as the intermediate state, the most intense band appears at 102 cm^{-1}, which is assigned as $D_0\beta OC_2H_5^1$. Shifting the whole spectrum to the left to make the $D_0\beta OC_2H_5^1$ band in Fig. 5(c) aligned with the origin 0^+ of the MATI spectra via $S_1 0^0$, it can

Table 4
Measured excitation energies and ionization energies of several benzene derivatives (unit: cm^{-1}).[a]

Molecule	E_1	ΔE_1	E_2	ΔE_2	IE	ΔIE	Reference
Benzonitrile	36 512	0	41 978	0	78 490	0	[6,28]
2-methoxybenzonitrile	34 176	−2336	36 482	−5496	70 658	−7832	[8]
2-ethoxybenzonitrile	34 092	−2420	35 704	−6274	69 796	−8694	This work
Benzene	38 086	0	36 471	0	74 557	0	[29,30]
Anisole	36 383	−1703	30 016	−6455	66 399	−8158	[31]
Phenetole	36 370	−1716	29 295	−7176	65 665	−8892	[5]

[a] ΔE_1, ΔE_2, and ΔIE are shifts of E_1, E_2 and IE with respect to benzonitrile or benzene.

be found that all the vibrational bands of Fig. 5(c) align well with those of Fig. 5(b) [13]. Therefore, MATI spectra via $S_1\beta OC_2H_5^1$ can be assigned as the combinations between $\beta OC_2H_5^1$ and the corresponding vibrations of MATI via $S_1 0^0$. No new fundamental mode was observed in MATI via $S_1\beta OC_2H_5^1$.

Fig. 5(d) shows the experimental MATI spectra via $S_1\nu OC_2H_5^1$ (320 cm^{-1}) and the most intense band appears at 340 cm^{-1}, which is assigned as $D_0\nu OC_2H_5^1$. Similarly, shifting the whole spectrum to the left to make the $\nu OC_2H_5^1$ band in Fig. 5(d) aligned with the 0^+ of the MATI spectra via $S_1 0^0$, it can be seen that the peaks in the higher frequency region than 340 cm^{-1} in Fig. 5(d) aligned well with the peaks in Fig. 5(b). Therefore, the spectra can also be assigned as the combinations between $\nu OC_2H_5^1$ and the corresponding vibrational modes of MATI spectra via $S_1 0^0$. The band at 327 cm^{-1} is assigned to the combination vibration $\gamma CN^1\gamma C_2H_5^1$ based on the spectral simulation.

All the vibrations found in the MATI spectrum are listed in Table 2. Most of them are related to the in-plane motion. When the vibration from OC_2H_5 is used as an intermediate state, a great deal of combination vibrations between OC_2H_5 and the ring vibration modes were observed.

3.4. Molecular structure in S_0, S_1, and D_0 states

Table 3 lists the geometric parameters of *trans*-2-ethoxybenzonitrile (conformer I) in the S_0, S_1, and D_0 states, calculated at B3LYP/aug-cc-pvtz level. From Table 3, it can be seen that every C—C bond of the ring become longer after the $S_1 \leftarrow S_0$ transition, and the circumference of the ring (sum of the six bond lengths) is increased by 0.13 Å. However, in the $D_0 \leftarrow S_1$ transition, the C—C bond length of the ring do not change consistently, some increase and some shorten, and ring circumference shortened by 0.06 Å. For all C—H bonds, bond length has no significant change. These are similar to other benzene derivative molecules [10,26,27]. The bond angle variation of the substituents is limited to the range of -3.0° – 2.5°, but the dihedral angles of the substituents do not any change. These indicate that there are great transition probabilities between the ground state S_0, excited state S_1 and ionic ground state D_0 owing to the similar molecular structures for these states, which is supported by strong REMPI and MATI signals. The variation of the aromatic ring during the transition leads to the activation of many in-plane vibrational modes.

3.5. Excitation and ionization energy

We list the excitation energies and the ionization energies of benzonitrile, 2-methoxybenzonitrile, 2-ethoxybenzonitrile, benzene, anisole, and phenetole in Table 4. It can be seen that different substitutions have a significant influence on the electronic transition energy. Both the methoxy and the ethoxy groups lead to a red shift of E_1 and E_2. The ethoxy group causes a slightly larger red shift than the methoxy group. It is known that the interactions between the substituent and the aromatic ring involve the conjugation (resonance) effect through the π orbital and the inductive effect through σ bond. The collective effect can give rise to a decrease in the zero-point energy level of the electronic state. If the interaction energy for the upper state is greater than for the lower state, the transition energy yields a red shift, conversely, causes a blue shift. The measured values in Table 4 indicate that the methoxy and ethoxy group have a greater interaction with the upper state than the lower state, and the interaction of the ethoxy group with the parent molecules is greater than that of the methoxy.

In general, electron-withdrawing group substitutions increase the ionization energy of parent molecule, while electron-donating groups decrease the ionization energy. In Table 4, the substitution of methoxy and ethoxy on ortho position of benzonitrile caused the IE to reduce by 7832 and 8694 cm^{-1}, respectively, while the substitution of methoxy and ethoxy of benzene caused the IE to reduce by 8158 and 8892 cm^{-1}, respectively. So, we can conclude that methoxy and ethoxy groups are of great electron-donating ability. Ethoxy is a stronger electron donor than methoxy. The IE of benzonitrile is about 3933 cm^{-1} higher than that of benzene, indicating that CN is an intense electron-withdrawing group.

4. Conclusion

The potential energy surface (PES) of ethoxybenzonitrile in the ground state was calculated at the level of B3LYP/cc-pvdz, and five different local minimums corresponding to five different molecular conformers were found on PES. Further structural optimizations and energy calculations for the ground state at the level of B3LYP/aug-cc-pvtz were performed to obtain the relative energies of five conformers included zero-point energy corrections to be 0, 600, 957, 1016, and 1306 cm^{-1}, respectively. Only the most stable conformer I (trans) was observed in the supersonic molecular beam experiment. The high-resolution vibrational spectra of the first electronically excited state S_1 and cationic ground state D_0 of 2-ethoxybenzonitrile were measured by two-color resonance enhanced multiphoton ionization (REMPI) and mass analyzed threshold ionization (MATI) spectroscopy. The band origin of $S_1 \leftarrow S_0$ transition and adiabatic ionization energies of 2-ethoxybenzonitrile are determined to be 34 092 ± 2 and 69 796 ± 5 cm^{-1}, respectively. The density functional theory calculations and Franck-Condon simulations were performed. The theoretical results are in good agreement with the experimental observations. The vibronic spectra for S_1 and D_0 states were analyzed in detail and assigned. The MATI spectra follow well the propensity rule $\Delta\nu = 0$, indicating that the molecular structure of the cationic ground is similar to that of the excited states. A lot of vibrational modes associated with ring in-plane distortion were observed.

Declaration of Competing Interest

The authors declare that they have no known competing financial interests or personal relationships that could have appeared to influence the work reported in this paper.

Data availability

No data was used for the research described in the article.

Acknowledgments

Project supported by National Natural Science Foundation of China (Grants Nos. 61835007, 12241408, 61575115), PCSIRT (No.

IRT_17R70), 111 project (Grant No. D18001), and the Fund for Shanxi "1331 Project" Key Subjects Construction.

Supplementary materials

Supplementary material associated with this article can be found, in the online version, at doi:10.1016/j.molstruc.2023.136278.

References

[1] G. Cinacchi, G. Prampolini, DFT Study of the Torsional Potential in Ethylbenzene and Ethoxybenzene: The Smallest Prototypes of Alkyl− and Alkoxy−Aryl Mesogens, J. Phys. Chem. A 107 (2003) 5228–5232, https://doi.org/10.1021/jp034648k.

[2] V. Ramanathan, P. Pandey, T. Chakraborty, Conformation and laser-induced fluorescence spectroscopy of phenetole in supersonic jet, Chem. Phys. Lett. 427 (2006) 18–23, https://doi.org/10.1016/j.cplett.2006.06.068.

[3] T. Egawa, D. Yamamoto, K. Daigoku, Conformational property of ethoxybenzene as studied by laser-jet spectroscopy and theoretical calculations, J. Mol. Struct. 984 (2010) 282–286, https://doi.org/10.1016/j.molstruc.2010.09.042.

[4] L. Ferres, W. Stahl, H.V.L. Nguyen, The molecular structure of phenetole studied by microwave spectroscopy and quantum chemical calculations, Mol. Phys. 114 (2016) 2788–2793, https://doi.org/10.1080/00268976.2016.1177217.

[5] N. Helle, I. Hintelmann, J. Grotemeyer, Detailed analysis of the vibronic structure of phenetole in its first excited state and ionic ground state, Eur. J. Mass Spectrom. 25 (2019) 142–156, https://doi.org/10.1177/1469066718822643.

[6] M. Araki, S. Sato, K. Kimura, Two-color zero kinetic energy photoelectron spectra of benzonitrile and its van der waals complexes with argon. Adiabatic ionization potentials and cation vibrational frequencies, J. Phys. Chem. 100 (1996) 10542–10546, https://doi.org/10.1021/jp960565a.

[7] E. Alejandro, A. Longarte, F.J. Basterretxea, F. Castano, J.A. Fernández, A REMPI and ZEKE-PFI study of 4-amino-3-ethylbenzonitrile, Chem. Phys. Lett. 425 (2006) 35–39, https://doi.org/10.1016/j.cplett.2006.05.040.

[8] Y. Zhao, Y.H. Jin, C.Y. Li, S.T. Jia, Two-color resonance enhanced two-photon ionization and mass analyzed threshold ionization spectroscopy of 2-methoxybenzonitrile, J. Mol. Spectrosc. 363 (2019), 111182, https://doi.org/10.1016/j.jms.2019.111182.

[9] Y.H. Jin, Y. Zhao, Y.G. Yang, L.R. Wang, C.Y. Li, S.T. Jia, Two-color resonance enhanced multi-photon ionization and mass analyzed threshold ionization spectroscopy of 2-aminobenzonitrile and the CN substitution effect, Chem. Phys. Lett. 692 (2018) 395–401, https://doi.org/10.1016/j.cplett.2017.12.073.

[10] N. Li, S.X. Li, L. Wang, H.H. Wang, Y.G. Yang, J.M. Zhao, C.Y. Li, Two-color resonance enhanced multiphoton ionization spectroscopy of o-hydroxybenzonitrile and Franck-Condon simulation, Acta Phys. Sin. 71 (2022), 023301, https://doi.org/10.7498/aps.71.20211659.

[11] C.Y. Li, M. Pradhan, W.B. Tzeng, Mass analyzed threshold ionization spectroscopy of p-cyanophenol cation and the CN substitution effect, Chem. Phys. Lett. 411 (2005) 506–510, https://doi.org/10.1016/j.cplett.2005.06.085.

[12] Y. Zhao, N. Li, S.Y. Dang, G.Q. Yang, C.Y. Li, Two-color resonance enhanced two-photon ionization and mass analyzed threshold ionization spectroscopy of pchlorobenzonitrile, Acta Phys. Sin. 71 (2022), 103301, https://doi.org/10.7498/aps.71.20220089.

[13] N. Li, S.X. Li, L. Wang, H.H. Wang, J.M. Zhao, C.Y. Li, Vibrational spectra of 2-cyanophenol cation studied by the mass analyzed threshold ionization technique, Chem. Phys. Lett 792 (2022), 139402, https://doi.org/10.1016/j.cplett.2022.139402, 2022.

[14] Y. Zhao, Y.H. Jin, J.Y. Hao, Y.G. Yang, L.R. Wang, C.Y. Li, S.T. Jia, Rotamers of p isopropylphenol studied by hole-burning resonantly enhanced multiphoton ionization and mass analyzed threshold ionization spectroscopy, Spectrochim. Acta A 207 (2019) 328–336, https://doi.org/10.1016/j.saa.2018.09.013.

[15] J.Y. Hao, C.Y. Duan, Y.G. Yang, C.Y. Li, S.T. Jia, Resonance enhanced two-photon ionization and mass analyzed threshold ionization spectroscopy of 4-ethylanisole, J. Mol. Spectrosc. 369 (2020), 111258, https://doi.org/10.1016/j.jms.2020.111258.

[16] Y. Zhao, Y.H. Jin, J.Y. Hao, Y.G. Yang, C.Y. Li, S.T. Jia, Resonance enhanced multiphoton ionization and mass analyzed threshold ionization spectroscopy of 4-fluorobenzonitrile, Chem. Phys. Lett. 711 (2018) 127–131, https://doi.org/10.1016/j.cplett.2018.09.039.

[17] C.Y. Duan, N. Li, Y. Zhao, C.Y. Li, Accurate determination of ionization energy of 1, 3-diethoxybenzene via photoionization efficiency spectrum in electrostatic field, Acta Phys. Sin. 70 (2021), 053301, https://doi.org/10.7498/aps.70.20201273.

[18] M.J. Frisch, G.W. Trucks, H.B. Schlegel, G.E. Scuseria, M.A. Robb, J.R. Cheeseman, G. Scalmani, V. Barone, G.A. petersson, H. Nakatsuji, X. Li, M. Caricato, A. V. Marenich, J. Bloino, B.G. Janesko, R. Gomperts, B. Mennucci, H.P. Hratchian, J. V. Ortiz, A.F. Izmaylov, J.L. Sonnenberg, D. Williams-Young, F. Ding, F. Lipparini, F. Egidi, J. Goings, B. Peng, A. Petrone, T. Henderson, D. Ranasinghe, V. G. Zakrzewski, J. Gao, N. Rega, G. Zheng, W. Liang, M. Hada, M. Ehara, K. Toyota, R. Fukuda, J. Hasegawa, M. Ishida, T. Nakajima, Y. Honda, O. Kitao, H. Nakai, T. Vreven, K. Throssell, J.A. Montgometry Jr., J.E. Peralta, F. Ogliaro, M. J. Bearpark, J.J. Heyd, E.N. Brothers, K.N. Kudin, V.N. Staroverov, T.A. Keith, R. Kobayashi, J. Normand, K. Raghavachari, A.P. Rendell, J.C. Burant, S.S. Iyengar, J. Tomasi, M. Cossi, J.M. Millam, M. Klene, C. Adamo, R. Cammi, J.W. Ochterski, R.L. Martin, K. Morokuma, O. Farkas, J.B. Foresman, D. J. Fox, Gaussian 16, Gaussian Inc., Wallingford CT, 2016.

[19] C.Y. Li, J.L. Lin, W.B. Tzeng, Mass-analyzed threshold ionization spectroscopy of the rotamers of p-n-propylphenol cation and configuration effect, J. Chem. Phys. 122 (2005), 044311, https://doi.org/10.1063/1.1839863.

[20] M. Schneider, M. Wilke, M.L. Hebestreit, J.A. Ruiz-Santoyo, L. Alvarez-Valtierra, J. T. Yi, W.L. Meerts, D.W. Pratt, M. Schmitt, Rotationally resolved electronic spectroscopy of the rotamers of 1, 3-dimethoxybenzene, Phys. Chem. Chem. Phys. 19 (2017) 21364–21372, https://doi.org/10.1039/c7cp04401a.

[21] L.W. Yuan, C.Y. Li, J.L. Lin, S.C. Yang, W.B. Tzeng, Mass analyzed threshold ionization spectroscopy of o-fluorophenol and o-methoxyphenol cations and influence of the nature and relative location of substituents, Chem. Phys. 323 (2006) 429–438, https://doi.org/10.1016/j.chemphys.2005.10.004.

[22] S.C. Yang, S.W. Huang, W.B. Tzeng, Rotamers of o- and m-dimethoxybenzenes studied by mass-analyzed threshold ionization spectroscopy and theoretical calculations, J. Phys. Chem. A 114 (2010) 11144–11152, https://doi.org/10.1021/jp1026652.

[23] M. Wilke, Mi. Schneider, J. Wilke, J.A. Ruiz-Santoyo, J.J. Campos-Amador, M. E. Gonzalez-Medina, L. Alvarez-Valtierra, M. Schmitt, Rotationally resolved electronic spectroscopy study of the conformational space of 3-methoxyphenol, J. Mol. Struct. 1140 (2017) 59–66, https://doi.org/10.1016/j.molstruc.2016.10.096.

[24] G. Varsanyi, Assignments of Vibrational Spectra of Seven Hundred Benzene Derivatives, Wiley, New York, 1974.

[25] E.B. Wilson, The normal modes and frequencies of vibration of the regular plane hexagon model of the benzene molecule, Phys. Rev. 45 (1934) 706–714, https://doi.org/10.1103/physrev.45.706.

[26] J. Huang, K.L. Huang, S.Q. Liu, Q. Luo, W.B. Tzeng, J. Photoch. Photobio. A 188 (2007) 252–259, https://doi.org/10.1016/j.jphotochem.2006.12.016.

[27] S.Y. Tzeng, K. Takahashi, W.B. Tzeng, Cation spectra of p-chloroanisole and the heavy atom effect on ionization energy, Chem. Phys. Lett. 731 (2019), 136626, https://doi.org/10.1016/j.cplett.2019.136626.

[28] K. Sakota, K. Nishi, K. Ohashi, H. Sekiya, Absence of dual fluorescence in jet-cooled benzonitrile and p-tolunitrile, Chem. Phys. Lett. 322 (2000) 407–411, https://doi.org/10.1016/S0009-2614(00)00420-6.

[29] L.A. Chewter, M. Sander, K. Müller-Dethlefs, E.W. Schlag, High resolution zero kinetic energy photoelectron spectroscopy of benzene and determination of the ionization potential, J. Chem. Phys. 86 (1987) 4737–4744, https://doi.org/10.1063/1.452694.

[30] R.G. Neuhauser, K. Siglow, H.J. Neusser, High nn Rydberg spectroscopy of benzene: Dynamics, ionization energy and rotational constants of the cation, J. Chem. Phys. 106 (1997) 896–907, https://doi.org/10.1063/1.473170.

[31] M. Pradhan, C.Y. Li, J.L. Li, W.B. Tzeng, Mass analyzed threshold ionization spectroscopy of anisole cation and the OCH3 substitution effect, Chem. Phys. Lett. 407 (2005) 100–104, https://doi.org/10.1016/j.cplett.2005.03.068.